

ChemComm

Accepted Manuscript



This article can be cited before page numbers have been issued, to do this please use: M. Bodiuzzaman, A. Nag, R. N. Pradeep, A. Chakraborty, R. Bag, P. Ganesan, G. Natarajan, G. Sekar, S. Ghosh and T. Pradeep, *Chem. Commun.*, 2019, DOI: 10.1039/C9CC01289C.



This is an Accepted Manuscript, which has been through the Royal Society of Chemistry peer review process and has been accepted for publication.

Accepted Manuscripts are published online shortly after acceptance, before technical editing, formatting and proof reading. Using this free service, authors can make their results available to the community, in citable form, before we publish the edited article. We will replace this Accepted Manuscript with the edited and formatted Advance Article as soon as it is available.

You can find more information about Accepted Manuscripts in the [author guidelines](#).

Please note that technical editing may introduce minor changes to the text and/or graphics, which may alter content. The journal's standard [Terms & Conditions](#) and the ethical guidelines, outlined in our [author and reviewer resource centre](#), still apply. In no event shall the Royal Society of Chemistry be held responsible for any errors or omissions in this Accepted Manuscript or any consequences arising from the use of any information it contains.



Journal Name

COMMUNICATION

A covalently linked dimer of $[\text{Ag}_{25}(\text{DMBT})_{18}]^-$

Mohammad Bodiuzzaman^a, Abhijit Nag^a, Raghu Narayanan Pradeep^a, Ankush Chakraborty^b, Ranjit Bag^b, Ganesan Paramasivam^a, Ganapati Natarajan^a Govindasamy Sekar^b, Sundargopal Ghosh^b and Thalappil Pradeep^{*a}

Received 00th January 20xx,
Accepted 00th January 20xx

DOI: 10.1039/x0xx00000x

We report the first example of a covalently bound dimer of monolayer protected atomically precise silver nanocluster, $[\text{Ag}_{25}(\text{DMBT})_{18}]^-$ (DMBT stands for 2,4-dimethylbenzenethiol). Covalently linked dimers could be important to design new cluster assembled materials with composite properties.

Atomically precise noble metal nanoclusters protected with ligands have emerged as a new research frontier in nanoscience, due to their unique optical and chemical properties as well as promising applications.¹⁻⁴ Out of these, the molecular systems studied in detail include $[\text{Au}_{102}(\text{p-MBA})_{44}]$, $[\text{Au}_{25}(\text{SCH}_2\text{CH}_2)_{18}]$, $[\text{Au}_{38}(\text{SCH}_2\text{CH}_2)_{24}]$, $[\text{Ag}_{44}(\text{p-MBA})_{30}]$, $[\text{Ag}_{25}(\text{SPhMe}_2)_{18}]$, $[\text{Ag}_{29}(\text{BDT})_{12}(\text{PPh}_3)_4]$, $[\text{Ag}_{40}(\text{SPhMe}_2)_{24}(\text{PPh}_3)_8]$, $[\text{Ag}_{46}(\text{SPhMe}_2)_{24}(\text{PPh}_3)_8]$ etc,⁵⁻¹² which exist in various charge states (the abbreviation used are presented in supplementary information). Single crystal X-ray diffraction has been utilized for their structural analysis while mass spectrometry is an important tool to understand their formulae and supramolecular interactions.^{13, 14} Dimers of $\text{Au}_{25}(\text{SR})_{18}$ (SR : phenyl ethanethiolate and butane thiolate) was first reported by our group using studies in the gas phase.¹⁵ This kind of dimers was not observed for structurally similar $[\text{Ag}_{25}(\text{DMBT})_{18}]^-$ clusters due to lack of metallophilic interactions.

Recently, synthesis of new superstructures by assembly of molecular pieces of metals has attracted great attention.¹⁶⁻¹⁸ The creation of superstructures by clusters without changing the original structure of the building block is a challenging task. Ligand exchange reaction is suitable in this regard and various studies have been done on gold clusters to create superstructures.^{16, 18} Ligands containing two reactive rigid thiol groups can be efficient to create the assembly of building blocks. This aspect of creating superstructures has not been explored in the case of silver nanoclusters.

In this communication, we demonstrate the synthesis of a covalently linked dimer of a monolayer protected cluster

(MPC), $[\text{Ag}_{25}(\text{DMBT})_{18}]^-$ by ligand-exchange reaction, wherein a complex of ruthenium bipyridyl-4-4'-dithiol $[\text{Ru}(\text{bpy})_2\text{bpy}(\text{CH}_2\text{SH})_2]^{2+}$ replaces two dimethylbenzenethiol ligands and creates a dimer. The products were characterized by optical absorption spectroscopy, infrared spectroscopy and detailed high resolution electrospray ionization mass spectrometry (HR ESI MS).

$[\text{Ag}_{25}(\text{DMBT})_{18}]^-$ and $[\text{Ru}(\text{bpy})_2\text{bpy}(\text{CH}_2\text{SH})_2](\text{PF}_6)_2$ were synthesized by following reported procedures^{6, 19} and characterized by optical absorption spectroscopy and HR ESI MS (Fig. S1 and S2). The ligand exchange reaction which leads to dimerization of $[\text{Ag}_{25}(\text{DMBT})_{18}]^-$ was carried out by mixing $[\text{Ru}(\text{bpy})_2\text{bpy}(\text{CH}_2\text{SH})_2]^{2+}$ and $[\text{Ag}_{25}(\text{DMBT})_{18}]^-$ in acetonitrile (see experimental section of supplementary information for details). The cleaned product obtained from the ligand exchange reaction was analysed by UV-vis spectroscopy. The optical absorption spectra of $[\text{Ag}_{25}(\text{DMBT})_{18}]^-$, its dimer and $[\text{Ru}(\text{bpy})_2\text{bpy}(\text{CH}_2\text{SH})_2]^{2+}$ are compared in Fig. 1. The spectrum of the dimer was changed slightly compared to the parent cluster from which we infer that the cluster core remains intact. There is a slight red shift of 600 nm and a change was observed near to 400 nm absorption which indicates optical coupling between $[\text{Ru}(\text{bpy})_2\text{bpy}(\text{CH}_2\text{SH})_2]^{2+}$ and the cluster. This type of minor changes in the optical absorption spectrum ensures that the building blocks are intact which is essential for creating superstructures.

HR ESI MS was used to show the formation of the dimer of $[\text{Ag}_{25}(\text{DMBT})_{18}]^-$. Sample preparation and instrumental details are given in supplementary information. Under optimized conditions for collecting the data, full range HR ESI MS shows two peaks, at m/z 5167 and m/z 5504. Expansion of the peak at m/z 5167 exhibits characteristic peak to peak separation of 1 which confirms its unit charge. This species is $[\text{Ag}_{25}(\text{DMBT})_{18}]^-$, confirmed by its perfect match of experimental and theoretical mass spectra. Similarly, the expanded peak at m/z 5504 shows the characteristic peak to peak separation of 0.5 which confirms its doubly charged state. This peak is assigned as the dimer of $[\text{Ag}_{25}(\text{DMBT})_{18}]^-$ linked by the $[\text{Ru}(\text{bpy})_2\text{bpy}(\text{CH}_2\text{SH})_2]^{2+}$ linker. The assignment of the peak was supported by the well matching of simulated and experimental isotopic distributions (Fig. 1). The presence of $[\text{Ag}_{25}(\text{DMBT})_{18}]^-$ in the full spectrum is

^aDepartment of Chemistry, DST Unit of Nanoscience (DST UNS) and Thematic Unit of Excellence (TUE), Indian Institute of Technology Madras, Chennai 600036, India,

^bDepartment of Chemistry, Indian Institute of Technology Madras, Chennai 600036, India. *E-mail: pradeep@iitm.ac.in

† Electronic Supplementary Information (ESI) available

COMMUNICATION

Journal Name

most likely to be due to the fragmentation of the dimeric species. This was further proven by collision induced dissociation experiment (CID). This experiment was performed by selecting the ion at m/z 5504 and colliding it at various

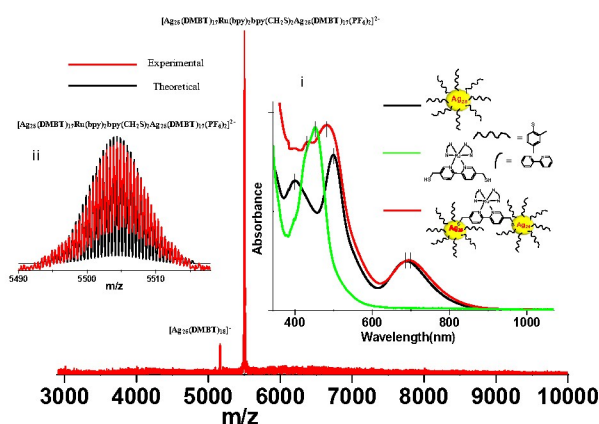


Fig. 1 Full range ESI MS in negative ion mode. The major peak at m/z 5504 is assigned as $[\text{Ag}_{25}(\text{DMBT})_{17}\text{Ru}(\text{bpy})_2\text{bpy}(\text{CH}_2\text{S})_2\text{Ag}_{25}(\text{DMBT})_{17}(\text{PF}_6)_2]^{2-}$. Comparison of the optical absorption spectra of Ag_{25} , its dimer and $[\text{Ru}(\text{bpy})_2\text{bpy}(\text{CH}_2\text{SH})_2]^{2+}$ is shown in inset (i). The features in the spectra are marked. The experimental isotopic distribution is compared with simulated spectrum in inset (ii). Red and black traces correspond to experimental and theoretical spectra, respectively.

laboratory collision energies. Upon increasing the laboratory collision energy (CE) from 0 to 30 V, the dimeric species is fragmented into monomeric species $[\text{Ag}_{25}(\text{DMBT})]^-$ and $[\text{Ru}(\text{bpy})_2\text{bpy}(\text{CH}_2\text{S})_2(\text{PF}_6)]^-$. Further increase in collision energy resulted in the formation of $[\text{Ag}_{22}\text{L}_{15}]^-$, $[\text{Ag}_{21}\text{L}_{14}]^-$, $[\text{Ag}_5\text{L}_6]^-$, and $[\text{Ag}_2\text{L}_3]^-$ (L correspond to DMBT) which is the regular fragmentation of $[\text{Ag}_{25}(\text{DMBT})_{18}]^-$ and this matches well with the previously reported fragmentation pattern.²⁰ Similar reactions were attempted by using only the dithiols, $[\text{Bpy}(\text{CH}_2\text{SH})_2]$, 1,4 BDT and biphenyl-4,4-dithiol but it was unsuccessful as after the mixing of dithiol and the cluster, the optical absorption spectra became featureless. It is likely to be due to the decomposition of $[\text{Ag}_{25}(\text{DMBT})_{18}]^-$ clusters (Fig. S3A-B).

The product was further analyzed by infrared spectroscopy (IR) to get further insights. IR spectra of the $[\text{Ru}(\text{bpy})_2\text{bpy}(\text{CH}_2\text{SH})_2]^{2+}$ and the cluster dimer were compared in Fig. S4 which revealed that the peak at wavenumber 2558 cm^{-1} is absent in the dimer. To get a clear view, the window of $2530\text{--}2580\text{ cm}^{-1}$ is expanded in Fig. S4. This region corresponds to the characteristic S-H frequency. This observation suggests that thiol group of $[\text{Ru}(\text{bpy})_2\text{bpy}(\text{CH}_2\text{SH})_2]^{2+}$ is linked with two clusters to form the dimer, by the loss of thiol protons. Similar experiments were performed with $[\text{Au}_{25}(\text{SR})_{18}]^-$ (SR : butane thiolate) but no dimer was observed. Upon addition of $[\text{Ru}(\text{bpy})_2\text{bpy}(\text{CH}_2\text{SH})_2]^{2+}$ to $[\text{Au}_{25}(\text{SR})_{18}]^-$ cluster solution, an instant colour change was observed and an oxidised feature of Au_{25} was observed in the UV-vis (Fig. S5D). We failed to get any signal in the ESI MS in negative ion mode but in positive ion mode, good intensity was observed at m/z 6527 which corresponds to $[\text{Au}_{25}(\text{BT})_{18}]^+$, (BT stands for 1-butanethiolate) confirmed by the perfect match of the theoretical and

experimental isotopic distributions. It is important to note that in both the ion modes, no peak was detected corresponding to $[\text{Ru}(\text{bpy})_2\text{bpy}(\text{CH}_2\text{SH})_2]$ in any charge state (Fig. S5A-C). Seemingly, instead of forming the dimer, electron transfer reaction has taken place. $[\text{Au}_{25}(\text{SR})_{18}]^-$ was oxidised to $[\text{Au}_{25}(\text{SR})_{18}]^+$ and consequently $[\text{Ru}(\text{bpy})_2\text{bpy}(\text{CH}_2\text{SH})_2]^{2+}$ was reduced to $[\text{Ru}(\text{bpy})_2\text{bpy}(\text{CH}_2\text{SH})_2]$. In order to check the influence of steric hindrance, similar experiments were performed with phenyl ethanethiol (PET) protected Au_{25} . In this case also, similar results were observed as discussed earlier. We have not studied the electron transfer process in detail as it is beyond the scope of this work.

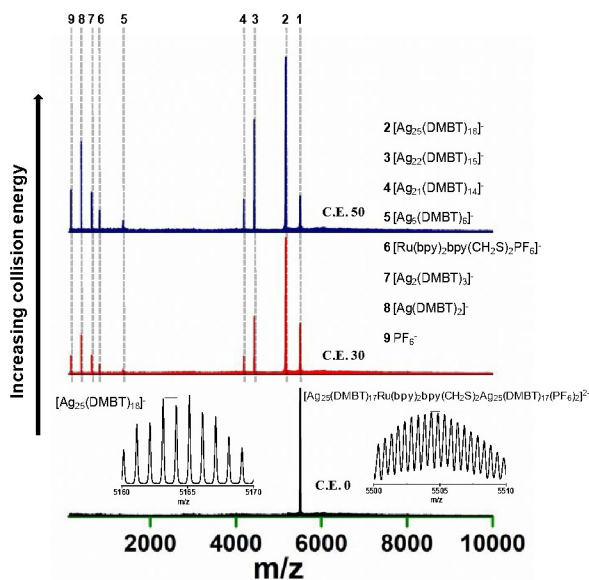


Fig. 2 Collision induced dissociation of m/z 5504 at various collision energies. With increasing collision energy, the species like $[\text{Ag}_{22}\text{L}_{15}]^-$, $[\text{Ag}_{21}\text{L}_{14}]^-$, $[\text{Ag}_5\text{L}_6]^-$, and $[\text{Ag}_2\text{L}_3]^-$ (L correspond to DMBT) were detected. All the fragments are marked and assigned. Most of the fragments are similar to the reported fragmentation of $[\text{Ag}_{25}\text{L}_{18}]^-$. The expansion of isotopic distributions of $[\text{Ag}_{25}\text{L}_{18}]^-$ and its dimer in 1- and 2- charge states show the characteristic peak to peak separation of m/z 1 and 0.5, respectively.

We were not able to grow single crystals of the dimer to get structural insights. However, powder X-ray diffraction of the dimer was performed and data are compared with the monomer in Fig. S6. The peaks shift to the lower side of 2θ in the dimer which reveals an increase in the interplanar distances (d). The extent of increase in d spacing is 5.2 \AA , comparable to the difference in ligand dimensions. The dimer was further characterized by SEM EDS to correlate the metal percentage in between Ru and Ag (Fig. S7). It shows the ratio of atomic percentage of Ag and Ru is $97.72 : 2.28 = 1 : 0.023$. This ratio is close (actual ratio, Ag: Ru = $1 : 0.02$) to the most probable composition of the dimer. To get further insights, the structure of the dimer was computed by density functional theory (DFT). The initial structure of $[\text{Ag}_{25}(\text{DMBT})_{18}]^-$ monomer was taken from its crystal structure and subsequently, it was optimized with complete ligands as well as using the reduced model ligands (Fig. S8A and S8B). Full theoretical details of the methods are given in supplementary information. The structure of $[\text{Ag}_{25}(\text{DMBT})_{18}]^-$ consists of an Ag_{13} icosahedral

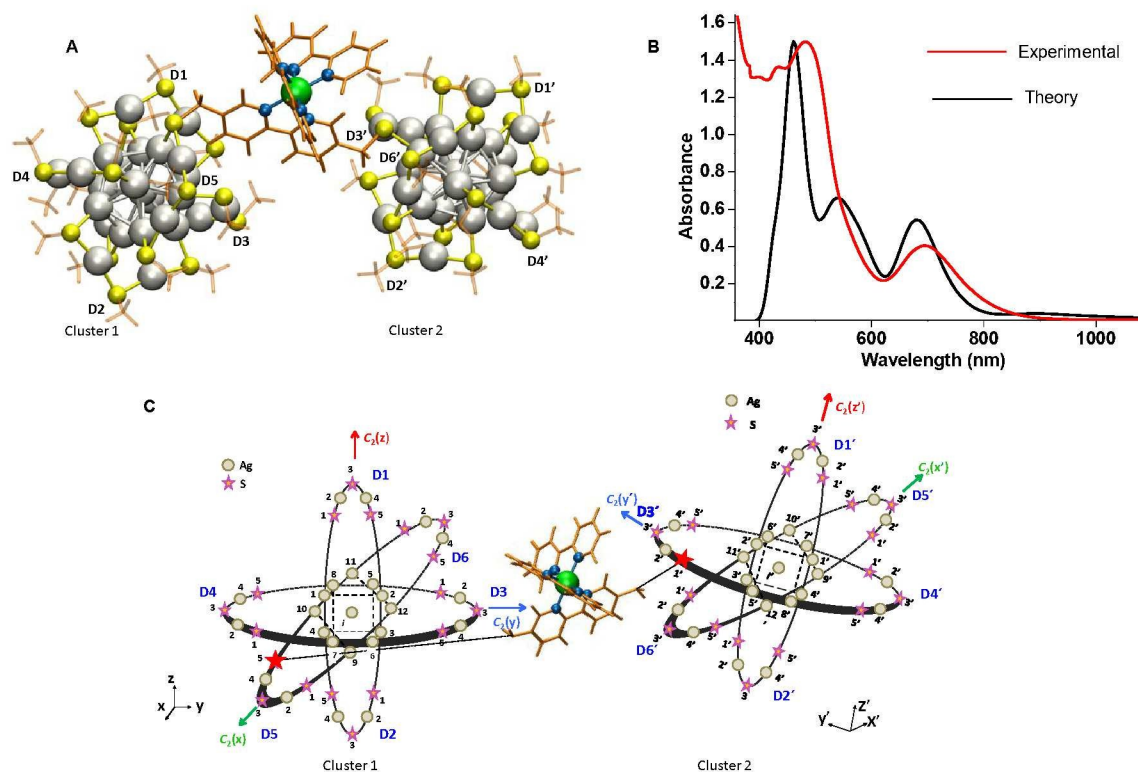


Fig. 3 (A) Density functional theory (DFT) optimized structure of the most stable isomer A of the dimer. Depending on the connectivity, different isomers were observed. (B) Optical spectrum of the most stable isomer was calculated by time-dependent DFT and it is compared with the experimental data. The comparison shows a reasonable match, particularly the 680 nm region. (C) The most stable isomer of the dimer in the aspicle (Borromean rings) representation. The bonding between $[\text{Ru}(\text{bpy})_2\text{bpy}(\text{CH}_2\text{SH})_2]^{2+}$ and $[\text{Ag}_{25}(\text{DMBT})_{18}]^{-}$ clusters are shown by dotted lines. The ligand sites, denoted by the locants (D5-5) and (D3'-1') marked by the larger red stars are those which are involved in the ligand exchange have been chosen on the basis of their calculated lower binding energies. Color code: gray, silver; blue, nitrogen; yellow, sulphur; green, ruthenium.

core, which is further covered by six $\text{Ag}_2(\text{SR})_3$ v-shaped staple units. Depending upon their location and connectivity, there are two different types of sulphur atoms. The two possible locations where ligand exchange can take place are i) at the apex sulphur atom of a staple and ii) at the sulphur atom between a staple silver atom and the inner icosahedral core silver atom (marked in Fig. S8C). We used the Borromean rings diagram and aspicle system of nomenclature²¹ to precisely identify binding sites and orientations of the clusters. Previous studies have shown that the sulphur locations ii are amenable for ligand exchange.²² This might be due to the weaker interactions of ligands present at these sites or due to the greater solvent accessible area in this region.²² Therefore, to find the appropriate locations for ligand exchange on the surface of $[\text{Ag}_{25}(\text{DMBT})_{18}]^{-}$ cluster, the linker molecule was connected to either cluster by replacing the ligands which are interacting between the staple and the inner icosahedral core atoms. The binding energy was obtained by subtracting the sum of energies of an isolated $[\text{Ag}_{25}(\text{DMBT})_{18}]^{-}$ cluster and the linker, $[\text{Ru}(\text{bpy})_2\text{bpy}(\text{CH}_2\text{SH})_2]^{2+}$ from the total energy of the complex, $[\text{Ag}_{25}(\text{DMBT})_{17}\text{Ru}(\text{bpy})_2\text{bpy}(\text{CH}_2\text{S})_2]^{+}$ and an isolated DMBT ligand. Based on the binding energies of the linker among three possible combinations of non-apex binding sites $\{(D5-5), (D3'-1')\}$, $\{(D5-5), (D2'-5')\}$ and $\{(D5-5), (D6'-1')\}$, (Fig. 3, see below), the sites with the higher binding affinity were

identified as being the most probable for the ligand exchange to form the dimer structure.

The lowest energy isomer of the dimer, A is shown in Fig. 3A. Structure of isomer A using Borromean rings diagram is shown in Fig. 3C. Full details of our method and the structures of other isomers are given in the supplementary information. We formed the dimer structure by attaching, via the linker molecule, cluster 1 (on the left in Fig. 3A) to a rotated and translated a copy of itself, which is referred to as cluster 2 (shown on the right in Fig. 3A). We first placed cluster 1 in standard orientation and labelled its locants. Next, we assigned the locants of cluster 2 and especially the sulphur locants required for describing the second binding site in the following way. We identified which sulphur atoms in each cluster are equivalent to each other, and thereby assigned similar aspicle locants to those sulphur atoms with primes used for locants on cluster 2. For example, the sulphur atom D3-1 in cluster 1 is equivalent to the sulphur atom D3'-1' in cluster 2 and so on.

Five possible isomers, A, B, C, D and E for the dimer structure were generated by connecting the site of the sulphur atom (D5-5) of the first cluster with three different sites of the second one as shown in Fig. S9. Isomers D and E have the same binding sites as isomers A and B, respectively, but slightly different conformations of the linker molecule. The energies of the five dimer structures (A-E) are given in the Table S2.

The most stable structure of the dimer, A was formed by the interaction of the linker between the sites (D5-5) and (D3'-1') of the $[\text{Ag}_{25}(\text{DMBT})_{18}]^-$ monomers (Fig. 3A and 3C). On the other hand, the dimer in isomer C links between the sites (D5-5) and (D2'-5') of the $[\text{Ag}_{25}(\text{DMBT})_{18}]^-$ clusters and exhibits least stability. Overall stability decreases in the order, $A < D < B < E < C$, where the locants of the linker binding are, $A = \{(D5-5), (D3'-1')\}$, $B = \{(D5-5), (D3'-1')\}$, $C = \{(D5-5), (D2'-5')\}$, $D = \{(D5-5), (D6'-1')\}$, $E = \{(D5-5), (D6'-1')\}$. The lowest energy isomer, A has fewer DMBT ligands close to the exchanged site on both clusters, which minimizes steric hindrance and thereby increases the conformational freedom of the linker. This leads to a closer inter-cluster distance, as measured between their central Ag atoms, and therefore, lowers total energy due to the decrease in steric hindrance and shorter atomic contacts between the linker atoms and the cluster ligand atoms. Besides the covalent linkage, there is a contribution of non-covalent interactions comprising the intercluster ligand-ligand van der Waals interactions. A π - π interaction was observed between the pyridyl groups and the phenyl groups of the DMBT ligand in the second lowest energy isomer, D. This implies that the orientation of clusters, the environment of the two exchange sites, and their associated degrees of steric hindrances play very important roles during the formation of such covalently-linked dimer structures. The total energy and aspicule locants (site position labels) of the sites of attachment of different isomers are presented in Fig. S9. Based on the structure computed, the aspicule name of the dimer is μ -(D5-5, D3'-1')-(5,5')-di(mercaptomethyl) ruthenium tris(bipyridine), di((DMBT)₁₇-argento-25 aspicule), where the binding sites on the clusters have been indicated in the prefix, and μ notation introduced here indicates the linker bridges the two clusters between the D5-5, sulphur site on cluster 1 and D3'-1' sulphur site on cluster 2, as shown in Fig. 3C. The binding sites of methyl groups of DMBT are omitted from this name for simplicity. The electronic and optical absorption properties were also studied using linear-response time dependent density functional theory (LR-TDDFT).²³ Electronic structures of monomer and dimer revealed that the transition taking place between the frontier orbitals in monomer is altered to deeper lying orbitals, especially the unoccupied levels. This implies that the linker plays a vital role in the electronic structure of the dimer. Bader charge analysis of the dimer and the monomer showed that the structural changes of the dimer are minor after the incorporation of the linker. Hence, it is clear that the alteration in the electronic structure of the dimer resulted changes in the UV/vis spectrum of the dimer (see supplementary information). Predicted spectrum of the most stable structure (Fig. 3B) showed a reasonable agreement with the experimental spectrum, which supports our calculated structure.

In conclusion, a covalently linked dimer of silver nanocluster was synthesised by a ligand exchange methodology. The formation of the dimer was confirmed by optical absorption spectroscopy, HR ESI MS and DFT. Theoretical prediction of the most stable binding site was made and identified using the aspicule positional notation and diagrams. It is worth noting

that the combined properties of the nanoclusters and chromophoric linker would be useful in the amplification of properties of individual constituents.

We thank the Department of Science and Technology for supporting our research project. M.B. thanks U. G. C. for his doctoral fellowship. A.N. and R.B. thank IITM for their fellowships. G.P. thanks IITM for an Institute Postdoctoral Fellowship.

Notes and references

- I. Chakraborty and T. Pradeep, *Chem. Rev.*, 2017, **117**, 8208-8271.
- R. Jin, C. Zeng, M. Zhou and Y. Chen, *Chem. Rev.*, 2016, **116**, 10346-10413.
- A. Mathew and T. Pradeep, *Part Part Syst Charact.*, 2014, **31**, 1017-1053.
- C. P. Joshi, M. S. Bootharaju and O. M. Bakr, *J. Phys. Chem. Lett.*, 2015, **6**, 3023-3035.
- P. D. Jadzinsky, G. Calero, C. J. Ackerson, D. A. Bushnell and R. D. Kornberg, *Science*, 2007, **318**, 430-433.
- C. P. Joshi, M. S. Bootharaju, M. J. Alhilal and O. M. Bakr, *J. Am. Chem. Soc.*, 2015, **137**, 11578-11581.
- L. G. AbdulHalim, M. S. Bootharaju, Q. Tang, S. Del Gobbo, R. G. AbdulHalim, M. Eddaoudi, D.-e. Jiang and O. M. Bakr, *J. Am. Chem. Soc.*, 2015, **137**, 11970-11975.
- M. J. Alhilal, M. S. Bootharaju, C. P. Joshi, T. M. Besong, A.-H. Emwas, R. Juarez-Mosqueda, S. Kaappa, S. Malola, K. Adil, A. Shkurenko, H. Häkkinen, M. Eddaoudi and O. M. Bakr, *J. Am. Chem. Soc.*, 2016, **138**, 14727-14732.
- H. Qian, W. T. Eckenhoff, Y. Zhu, T. Pintauer and R. Jin, *J. Am. Chem. Soc.*, 2010, **132**, 8280-8281.
- H. Yang, Y. Wang, H. Huang, L. Gell, L. Lehtovaara, S. Malola, H. Häkkinen and N. Zheng, *Nat. Commun.*, 2013, **4**, 2422.
- B. Mohammad, A. Ghosh, K. S. Sugi, A. Nag, E. Khatun, B. Varghese, G. Paramasivam, S. Antharjanam and G. Natarajan and T. Pradeep, *Angew. Chem. Int. Ed.*, 2019, **58**, 189-194.
- J. Chai, S. Yang, Y. Lv, T. Chen, S. Wang, H. Yu and M. Zhu, *J. Am. Chem. Soc.* 2018, **140**, 15582-15585.
- A. Mathew, G. Natarajan, L. Lehtovaara, H. Häkkinen, R. M. Kumar, V. Subramanian, A. Jaleel and T. Pradeep, *ACS Nano*, 2014, **8**, 139-152.
- A. Nag, P. Chakraborty, G. Paramasivam, M. Bodiuzzaman, G. Natarajan and T. Pradeep, *J. Am. Chem. Soc.*, 2018, **140**, 13590-13593.
- A. Baksi, P. Chakraborty, S. Bhat, G. Natarajan and T. Pradeep, *Chem. Commun.*, 2016, **52**, 8397-8400.
- T. Lahtinen, E. Hulkko, K. Sokolowska, T.-R. Tero, V. Saarnio, J. Lindgren, M. Pettersson, H. Häkkinen and L. Lehtovaara, *Nanoscale*, 2016, **8**, 18665-18674.
- A. Sels, G. Salassa, F. Cousin, L.-T. Lee and T. Bürgi, *Nanoscale*, 2018, **10**, 12754-12762.
- R. Ho-Wu, K. Sun and T. Goodson, *J. Phys. Chem. C*, 2018, **122**, 2315-2329.
- P. Bertoncello, E. T. Kefalas, Z. Pikramenou, P. R. Unwin and R. J. Forster, *J. Phys. Chem. C*, 2006, **110**, 10063-10069.
- P. Chakraborty, A. Baksi, E. Khatun, A. Nag, A. Ghosh and T. Pradeep, *J. Phys. Chem. C*, 2017, **121**, 10971-10981.
- G. Natarajan, A. Mathew, Y. Negishi, R. L. Whetten and T. Pradeep, *J. Phys. Chem. C*, 2015, **119**, 27768-27785.
- C. L. Heinecke, T. W. Ni, S. Malola, V. Mäkinen, O. A. Wong, H. Häkkinen and C. J. Ackerson, *J. Am. Chem. Soc.*, 2012, **134**, 13316-13322.
- M. Walter, H. Häkkinen, L. Lehtovaara, M. Puska, J. Enkovaara, C. Rostgaard and J. J. Mortensen, *J. Chem. Phys.*, 2008, **128**, 244101/244101-244101/244110.

COMMUNICATION

Journal Name

Published on 02 April 2019. Downloaded by UNIVERSITE PARIS SUD on 4/2/2019 10:37:30 AM.

ChemComm Accepted Manuscript